



Convective heat transfer from a heated elliptic cylinder at uniform wall temperature

Kaprawi S., Dyos Santoso

Mechanical Department of Sriwijaya University, Jl. Raya Palembang-Prabumulih Km. 32 Inderalaya
50062 Ogan Ilir, Indonesia.

Abstract

This study is carried out to analyse the convective heat transfer from a circular and an elliptic cylinders to air. Both circular and elliptic cylinders have the same cross section. The aspect ratio of cylinders range $0 \leq \varepsilon \leq 1$ are studied. The implicit scheme of the finite difference is applied to obtain the discretized equations of hydrodynamic and thermal problem. The Choleski method is used to solve the discretized hydrodynamic equation and the iteration method is applied to solve the discretized thermal equation. The circular cylinder has the aspect ratio equal to unity while the elliptical cylinder has the aspect ratio less than unity by reducing the minor axis and increasing the major axis to obtain the same cross section as circular cylinder. The results of the calculations show that the skin friction change significantly, but in contrast with the elliptical cylinders have greater convection heat transfer than that of circular cylinder. Some results of calculations are compared to the analytical solutions given by the previous authors.

Copyright © 2013 International Energy and Environment Foundation - All rights reserved.

Keywords: Forced convection; Flow; Elliptic cylinder; Aspect ratio; Heat transfer.

1. Introduction

Heat transfer by forced convection flows initiated impulsively occur naturally in the environment and can be implicated in many industrial applications. Well-documented examples of these flows include impulsively generated forced convection from horizontal cylindrical bodies. Numerous numerical, experimental and theoretical studies devoted to these cases have appeared in the literature over the years. Johnson et al. studied analytically the flow around an elliptical cylinder by using 2D spectral-element method to solve the unsteady Navier-Stokes equations governing the fluid flow [1]. Simulations were carried out for aspect ratios from 0.01 to 1.00 and Reynolds numbers from 30 to 200. The flow is perpendicular to a which is always longer than b and they defined as $\varepsilon = b/a$. The results show that the drag coefficients vary in function of aspect ratio which is larger than drag coefficient of a circular cylinder or $C_d > 1.2$.

Recently, forced convection from a circular cylinder ($\varepsilon = 1$) was studied analytically by Khan et al. [2]. They give the evolution of shear stress and drag coefficient of flow around a circular cylinder and average Nusselt number. The calculations are compared to the previous authors. Khan et al. studied analytically heat transfer and flow around an elliptic cylinder in the high Reynolds number range of 10^2 to 10^5 [3]. The aspect ratios of elliptical cylinder studied are 2, 3 and 4. The results show that the drag coefficients are lower whereas the average heat transfer coefficient are higher for elliptical cylinder than that of circular cylinder. Alessio et al. give numerical solution of Navier-Stokes and energy equation

using a spectral finite difference procedure [4]. The elliptic cylinder makes an angle of attack to the flow direction. They show that Nusselt number varies with time.

The skin friction drag of flow around an elliptic cylinder is numerically calculated by using commercial software by Sivakumar et al. in two-dimensional steady cross-flow regime for the range of Reynolds number as $0.01 \leq Re \leq 40$, aspect ratio as $0.2 \leq \varepsilon \leq 5$ [5]. The results show that the skin friction drag increases with aspect ratio.

Bharti et al. give the complete studies of heat transfer by convection from an elliptic cylinder for wide range of aspect ratio ($0.2 \leq \varepsilon \leq 5$) [6]. They used commercial software to obtain convection heat transfer to incompressible power-law fluids from a heated elliptic cylinder in the steady, laminar cross-flow regime. They show that for elliptic cylinder ($\varepsilon < 1$) the heat transfer is higher than that of circular cylinder, and if $\varepsilon > 1$ the heat transfer from an elliptical cylinder is lower than that of circular cylinder.

Extensive numerical simulations of the 2D laminar flow of power-law fluids over elliptic cylinders with different aspect ratios have been carried out to establish the conditions for the onset of wake formation and the onset of vortex shedding. This study was done by Koteswara et al. [7]. The continuity and momentum equations were solved numerically using commercial software. Velocity vector plots denoting the flow separation and vortices profiles showing the vortex shedding are also included. The flow field around a streamlined body can be well approximated by a potential flow field since viscous effects are confined to a thin boundary layer and wake [8].

Hayati et al. [9] give the prediction convective heat transfer from elliptical cylinder tube influenced by walls of both sides which has variable distance from the elliptic cylinder. The major axis of the elliptic cylinder is parallel to the walls. The heat transfer is maximum when the distance is about three times larger than the minor axis of elliptical tube.

The studies explained above did not confirm the same cross section for all aspect ratio of elliptic cylinders. In fact by changing the aspect ratio of a circular cylinder may cause the cross section or surface is not the same as circular cylinder. The aspect ratio of an elliptic cylinder is varied by changing one of the axis i.e. minor or major axis. Thus this study is to observe the heat transfer by forced convection of a circular cylinder and an elliptic cylinder of which both cylinders have the same cross section. The elliptic cylinders have the aspect ratio in the range of $0 \leq \varepsilon \leq 1$. If $\varepsilon = 0$ and $\varepsilon = 1$ the cylinder behaves as a flat plate and circular cylinder respectively. Some results are compared to the previous works.

2. Governing equations

Consider the two-dimensional, laminar, steady flow of an incompressible fluid with a uniform velocity and temperature (U_o, T_o) across an infinitely long cylinder of elliptic cross-section (aspect ratio, $\varepsilon = b/a$). The surface of the cylinder is maintained at a constant temperature, $T_w (> T_o)$. The thermo-physical properties of the streaming fluid are assumed to be independent of the temperature and the viscous dissipation effects are neglected. The flow is simulated by enclosing an isothermal elliptic, region from surface of cylinder to the boundary as shown schematically in Figure 1. But the domain of calculation is on the upper part region due to the symmetry.

The potential flow velocity just outside the boundary layer is denoted by $U(x)$. Using the order-of-magnitude analysis, the reduced equations of continuity, momentum and energy in the curvilinear system of coordinates in Figure 1 can be written as;

Continuity:

$$\frac{\partial u}{\partial x} + \frac{\partial v}{\partial y} = 0 \quad (1)$$

x-momentum:

$$u \frac{\partial u}{\partial x} + v \frac{\partial u}{\partial y} = -\frac{1}{\rho} \frac{dp}{dx} + \nu \frac{\partial^2 u}{\partial y^2} \quad (2)$$

Energy:

$$u \frac{\partial T}{\partial x} + v \frac{\partial T}{\partial y} = \lambda \frac{\partial^2 T}{\partial y^2} \quad (3)$$

Bernoulli equation:

$$-\frac{1}{\rho} \frac{dp}{dx} = U(x) \frac{dU}{dx} \quad (4)$$

$U(x)$ is formulated by Khan et al. [3]. The above equations of momentum and energy are subject to the following boundary conditions. At the cylinder surface (uniform wall temperature),

i.e., at $y = 0$: $u = v = 0$, $T = T_w$

At the edge boundary layer, i.e., at $y = \delta(x)$: $u = U(x)$, $T = T_\infty$

The equations (1), (2), and (3) may be transformed to dimensionless form as follows:

$$u^+ \frac{\partial u^+}{\partial x^+} + v^+ \frac{\partial u^+}{\partial y^+} = U^+ \frac{dU^+}{dx^+} + \frac{\partial^2 u^+}{\partial y^{+2}} \quad (5)$$

$$\frac{\partial u^+}{\partial x^+} + \frac{\partial u^+}{\partial y^+} = 0 \quad (6)$$

$$u^+ \frac{\partial T^+}{\partial x^+} + v^+ \frac{\partial T^+}{\partial y^+} = \frac{1}{Pr} \frac{\partial^2 T^+}{\partial y^{+2}} \quad (7)$$

with $x^+ = x/d$, $y^+ = Re^{1/2} y/d$, $u^+ = u/U_o$, $v^+ = Re^{1/2} v/U_o$, $p^+ = P/\rho U_o^2$, $T^+ = (T - T_\infty)/(T_w - T_\infty)$, $U^+ = U(x)/U_o$, $Re = U_o d/\nu$.

Boundary conditions become:

at the cylinder surface: $u^+ = v^+ = 0$, $T^+ = 1$

at the edge of boundary layer: $u^+ = U^+(x)$, $T^+ = 0$

The wall friction and convective heat transfer occur significantly from stagnation point to the separation point of the flow at the cylinder surface. Skin friction drag is due to viscous shear forces produced at the cylinder surface, predominant in those regions where the boundary layer is attached. In dimensionless form, C_f can be written as

$$C_f = \frac{\tau_w}{\frac{1}{2} \rho U_o^2} = \frac{\mu (\partial u / \partial y)_{y=0}}{\frac{1}{2} \rho U_o^2} \quad (8)$$

For a cylinder in dimensionless form, the average skin friction coefficient is

$$C_F = \frac{2}{Re^{1/2}} \int_0^{x_s^+} \left(\frac{\partial u^+}{\partial y^+} \right)_{y=0} dx^+ \quad (9)$$

The local Nusselt number is written as

$$Nu_x = \frac{q_w x}{(T_w - T_\infty)} = - \frac{d(\partial T / \partial y)_{y=0}}{(T_w - T_\infty)} \quad (10)$$

and then the average Nusselt number is calculated by integrating the local values over the length of the cylinder or by dimensionless form is as follows;

$$N_u = Re^{1/2} \int_0^{x_s^+} \left(\frac{dT^+}{dy^+} \right)_{y^+=0} dx_s^+ \quad (11)$$

with x_s^+ is dimensionless length of cylinder wall from stagnation point to the separation point.

The work presented here is focussed on the flow field around a cylinder and the convective heat transfer from a cylinder to the air in which the cylinder wall temperature is uniform. Starting from a circular cylinder ($\epsilon = 1$) the aspect ratio is changed to $\epsilon < 1$. These changes make the circular cylinder become an elliptical cylinder and both circular and elliptical cylinder have the same cross section.

3. Method of solution

By using the finite difference method with implicit scheme [10, 11], the equation (5) becomes

$$u_{i,j}^+ \frac{u_{i+1,j}^+ - u_{i,j}^+}{\Delta x^+} + v_{i,j}^+ \frac{u_{i,j+1}^+ - u_{i,j-1}^+}{2\Delta y^+} = \frac{U_{i+1}^{+2} - U_i^{+2}}{2\Delta x^+} + \frac{u_{i+1,j+1}^+ - 2u_{i+1,j}^+ + u_{i+1,j-1}^+}{\Delta y^{+2}} \tag{12}$$

and after regrouping we have the following equation;

$$a_i u_{i+1,j+1}^+ + b_i u_{i+1,j}^+ + c_i u_{i+1,j-1}^+ = d_i \tag{13}$$

with a_i, b_i, c_i and d_i are the coefficients of equation and subscript i, j are grid point number in x and y direction respectively. The continuity equation (6) is written in the finite difference scheme by using the forward difference for the term in x direction and the central difference for the term in normal direction. This equation allows to calculate the velocity in normal direction, $v_{i,j}^+$.

The energy equation (7) is written by using the finite difference method and we have

$$u_{i,j}^+ \frac{T_{i+1,j}^+ - T_{i,j}^+}{\Delta x^+} + v_{i,j}^+ \frac{T_{i,j+1}^+ - T_{i,j-1}^+}{2\Delta y^+} = \frac{1}{Pr} \frac{T_{i,j+1}^+ - 2T_{i,j}^+ + T_{i,j-1}^+}{\Delta y^{+2}} \tag{14}$$

and after regrouping we have the energy equation as follows

$$e_i T_{i+1,j+1}^+ + f_i T_{i+1,j}^+ + g_i T_{i+1,j-1}^+ = h_i \tag{15}$$

with e_i, f_i, g_i and h_i are the coefficients of equation

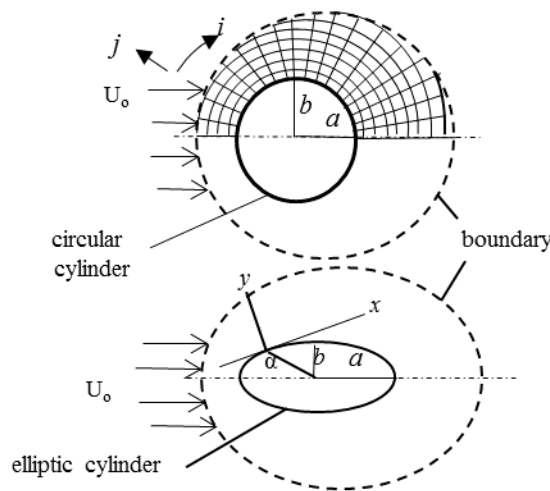


Figure 1. Numerical grid

The linearized equation, Eq. (13), makes tridiagonal matrix which is solved by Choleski method to obtain velocity distributions, $u_{i,j}^+$ and the linear equation, Eq. (15), is solved by Gauss-Seidel iteration method to obtain temperature distributions, $T_{i,j}^+$. The numerical grid where (i, j) is a typical mesh point (Figure 1). Outside the cylinder wall, mesh point are numbered consecutively with the i progressing in the meridional direction with $i = 1, 2, 3, \dots, m$ from the stagnation point. The j is progressing in the radial

direction starting from $j = 1$ on the cylinder's surface till $j = n$ in the external flow boundary. The computations were performed for grid points of 50×50 . Larger numbers of grids were used in meridional direction for smaller aspect ratio to obtain Δx constant and also in normal direction where the grid point is progressing from the stagnation point. The length of normal distance increases with x^+ from stagnation point (boundary as shown in Figure 1) because the boundary layer thickness increases with x . The absolute convergence of iteration is less than 10^{-5} for all cases.

4. Results and discussion

The numerical calculations were carried out for some values of aspect ratio. The length of circular cylinder surface in meridional direction ($\varepsilon = 1$) has the same length of elliptic cylinders when the aspect ratios $\varepsilon = 0, 0.361$ and 0.616 . When $\varepsilon = 0$ the circular cylinder become a flat plate in which the boundary condition is changed in calculation because the pressure gradient is zero. The value of Pr is taken to be 0.70 which correspond physically to air. Figure 2 (a) and (b) present two examples of typical velocity profiles for $\varepsilon = 0.361$ and $\varepsilon = 1$. We see that the velocity distributions for different aspect ratio are similar. The difference of velocity profiles for different aspect ratios are the values of velocity, the slope of velocity in laminar sublayer and the boundary layer thickness. We observe that the velocity and the slope increase with the rise of aspect ratio but the boundary layer thickness decrease with the increase of aspect ratio. The above conditions are due to higher pressure gradient when aspect ratio is higher.

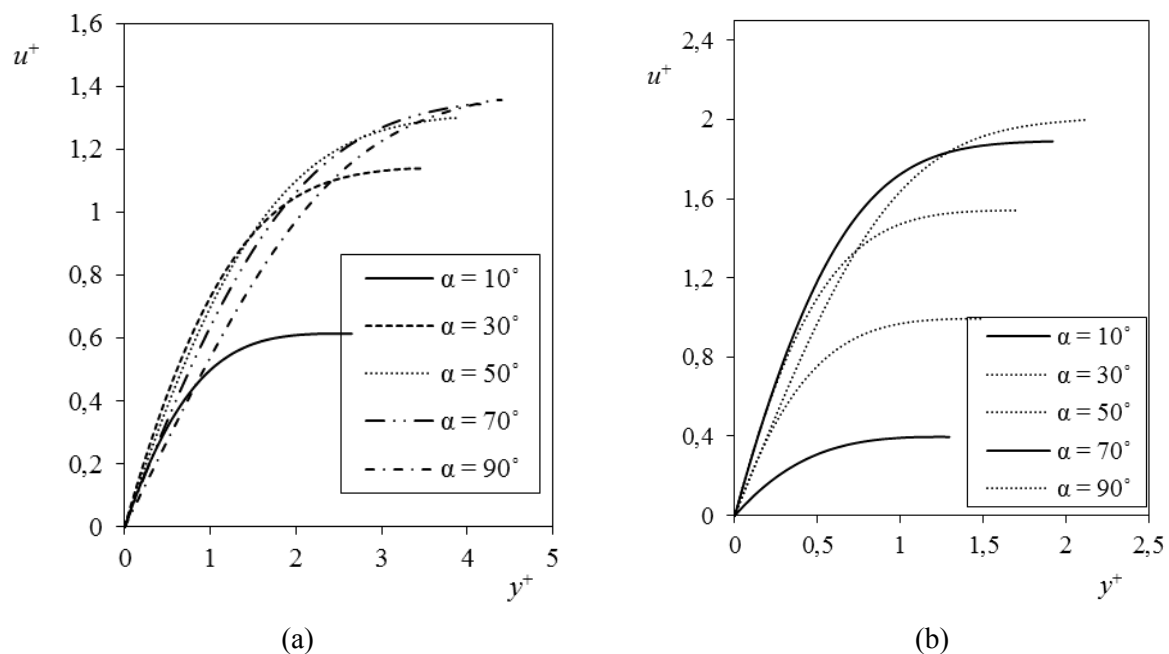


Figure 2. Velocity profiles (a) $\varepsilon = 0.361$ (b) $\varepsilon = 1$

Local skin friction coefficient is presented in Figure 3. The coefficient vary with α and it is a represe of velocity near the wall. It can be observed that the point of maximum value occurs at $\alpha = 59.5^\circ$ for $\varepsilon = 1$ (circular cylinder) and skin friction profile is almost practically symmetric. For $\varepsilon = 0.361$ and 0.616 the skin frictions increase rapidly with α and then reach maximum values at $\alpha = 41.3^\circ$ for $\varepsilon = 0.616$ and $\alpha = 25.2^\circ$ for $\varepsilon = 0.361$. It means that the maximum skin friction approach the stagnation point if the aspect ratio is decreased. At the rear part of cylinder, the velocity near the wall decrease with α and equal to zero at the point of separation. The position of separation point is far from the stagnation point with decreasing of aspect ratio. According to our result of numerical calculations, the separation points occured on cylinder wall are at $\alpha = 109.43^\circ$, $\alpha = 118.27^\circ$ and $\alpha = 132.35^\circ$ for $\varepsilon = 1$, $\varepsilon = 0.616$ and $\varepsilon = 0.361$ respectively. The skin friction calculation for circular cylinder is compared with previous result given by Khan et al [3] and the result is in good agreement because the difference is less than one percent. (Figure 3).

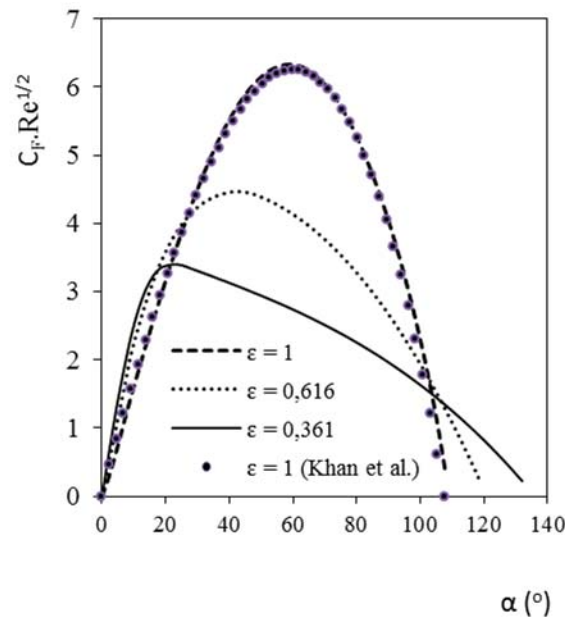


Figure 3. Local skin friction coefficient

The average value of skin friction coefficient is shown in Figure 4. The skin friction increase significantly with increase of aspect ratio. According to our calculations, if $\varepsilon = 0$ the cylinder behaves as a flat plate which has skin friction coefficient $C_F = 1.236/Re^{1/2}$. This value has small difference with that calculated analytically in most literature for flat plate which has skin friction coefficient $C_F = 1.292/Re^{1/2}$. For circular cylinder ($\varepsilon = 1$) from Figure 4 give that $C_F = 5.807 Re^{1/2}$. When this value is compared to the value given analytically by Khan et al who gave $C_F = 5.786 Re^{1/2}$ [2]. The difference is less than 1% which is acceptable.

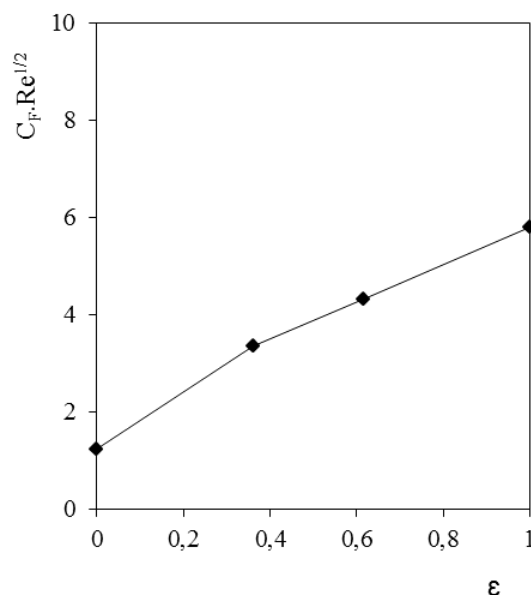


Figure 4. Average skin friction coefficient

The example of temperature characteristics is given by Figure 5 for $\varepsilon = 0.361$ and $\varepsilon = 1$. In various positions from stagnation point (different α), it is noticed that the temperature starts at the same temperature ($T^+ = 1$) at the cylinder surface and then temperature decrease with y^+ . Far from surface, the temperature all converge to the same value in free stream i.e zero at edge of boundary layer as prescribed by boundary condition there. It is also noticed that the temperature difference are significant for small

aspect ratio in various α and if the aspect ratio increase the temperature differences decrease because velocity increase when aspect ratio increase or boundary layer thickness is smaller for ϵ increase. The properties of thermal boundary layer are similar to that of hydrodynamic boundary layer in which the thermal boundary thickness decreases if aspect ratio increases.

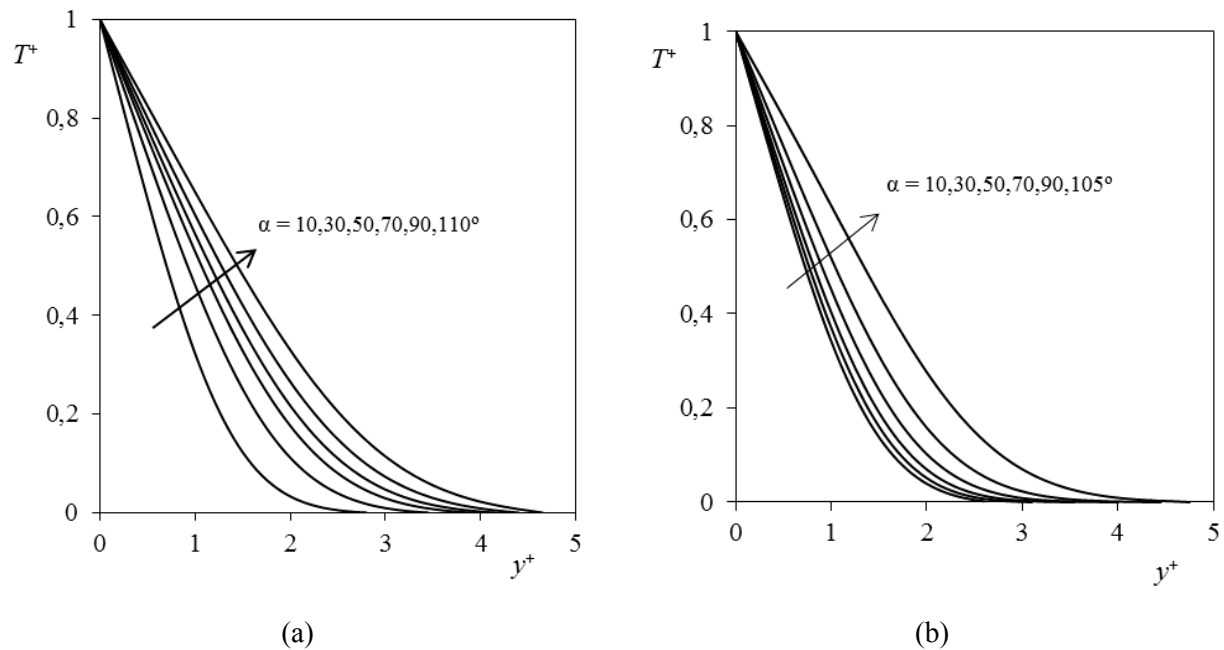


Figure 5. Temperature profiles (a) $\epsilon = 0,361$ and (b) $\epsilon = 1$

The convective heat transfer in terms of average Nusselt number is presented in Figure 6. It can be observed that starting from circular cylinder ($\epsilon = 1$), the Nusselt number increase with decrease of ϵ . It shows that the variations of circular cylinder to the elliptic cylinder in maintaining the same surface area makes the Nusselt number increase. The elliptic cylinder has better forced convective heat transfer than circular cylinder. Thus the geometry of streamline elliptic cylinders makes the separation point occur far from stagnation point.

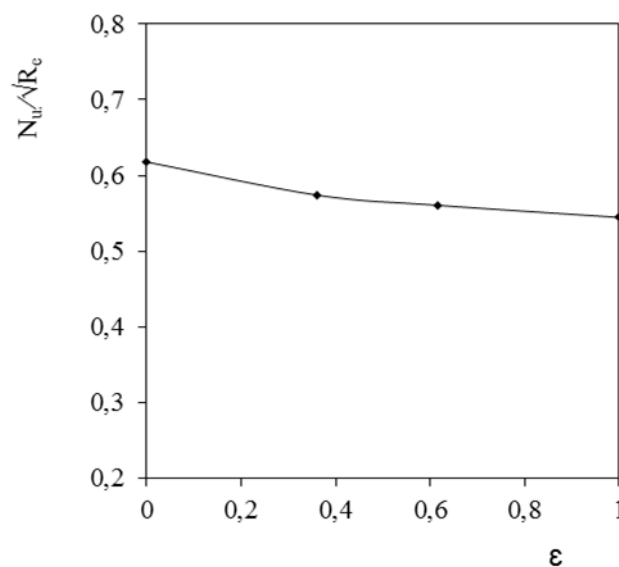


Figure 6. Average Nusselt number

The analytical solution for circular cylinder ($\epsilon = 1$) given by Khan et al. [3] is $N_u = 0.593Re^{1/2}Pr^{1/3}$ while for flat plate $N_u = 0.664Re^{1/2}Pr^{1/3}$. The present calculation gives for circular cylinder $N_u/Re^{1/2} = 0.545$ and for flat plate $N_u/Re^{1/2} = 0.617$. The difference between the previous and the present calculations is about 2.5% which is still in acceptable tolerance.

5. Conclusion

The convective heat transfer from the circular and the elliptic cylinder has been studied numerically by using the finite difference scheme. It is important to be concluded that the heat transfer from the elliptic cylinder ($0 < \epsilon < 1$) has better than that of the circular cylinder. It is noted that in this case, the circular and the elliptic cylinders both have the same cross section.

References

- [1] S.A Johnson, M.C. Thompson, K. Hourigan, Flow Past Elliptic Cylinders at Low Reynolds Numbers, 14th Australasian Fluid Mechanics Conference Adelaide University, Adelaide, Australia, 12-14, 2011.
- [2] W.A. Khan, J.R. Culham, M.M. Yovanovich, Fluid Flow Around and Heat Transfer From an infinite Circular Cylinder, Journal of Heat Transfer, Vol. 127, 2004.
- [3] W.A. Khan, J.R. Culham, M.M. Yovanovich, Fluid Flow around and Heat Transfer from Elliptic Cylinders : Analytical Approach, Journal of Thermophysics and Heat Transfer, Vol. 19, No. 2, 2005.
- [4] S.J.D. Alessio, M.G. Saunders, D.L. Harmsworth, Forced and mixed convective heat transfer from accelerated flow past an elliptic cylinder, International Journal of Heat and Mass Transfer, Vol. 46, p. 2927–2946, 2003.
- [5] P. Sivakumar, R.P. Bharti, R.P. Chhabra, Steady flow of power-law fluids across an unconfined elliptic cylinder, Journal of Chemical Engineering Science, Vol. 62, p.1682 – 1702, 2007.
- [6] R.P. Bharti, P. Sivakumar, R.P. Chhabra, Forced convection heat transfer from an elliptic cylinder to power-law fluids, International Journal of Heat and Mass Transfer, Vol. 51 p.1838–1853, 2008.
- [7] P. Koteswara Rao, K. Akhilesh, R.P. Chhabra, Flow of Newtonian and Power-Law Fluids Past an elliptic Cylinder : A Numerical Study, Ind. Eng. Chem. Res., 49, p. 6649–6661, 2010.
- [8] B. Turnbull B., J.N Mc Elwaine, Potential flow models of suspension current air pressure, Annals of Glaciology 51(54), 2010.
- [9] M. Hayati, Baharal Akhlaaghi and Maysam Azizi, Prediction of Natural Convection heat Transfer from a confined Horizontal elliptic tube using using Radial basic Function Network, International Journal of Research and Reviews in Applied Sciences, Volume 2, Issue 1, 2010.
- [10] F.M. White, Viscous Fluid Flow, 3rd edition, Mc Graw-Hill, p. 272-287, 2006.
- [11] J.P. Nougier, Méthodes de calcul numérique, 2e édition, Masson, Paris, p.240-243, 1985.



Kaprawi S. is professor at the Department of Mechanical Engineering, Sriwijaya University INDONESIA. His main research interests are fluid flow and heat & mass transfer, and fluid machineries.
E-mail address: kaprawi@unsri.ac.id



Dyos Santoso is master of Engineering in Mechanical Engineering. He is lecturer in Department of Mechanical Engineering, Sriwijaya University INDONESIA. His main research interest are fluid machineries, exergy analysis and heat transfer.
E-mail address: dyos_santoso@yahoo.com